On the role of hydrogen bond exchanges in the spectral diffusion of water

Zeke A. Piskulich,[1] Damien Laage,[2, a)] and Ward H. Thompson[1, b)]
[1)] *Department of Chemistry, University of Kansas, Lawrence, KS 66045, USA*
[2)] *PASTEUR, Department of Chemistry, École Normale Supérieure, PSL University, Sorbonne Université, CNRS, 75005 Paris, France*

(Dated: 1 June 2021)

The dynamics of a vibrational frequency in a condensed phase environment, *i.e.*, the spectral diffusion, has attracted considerable interest over the last two decades. A significant impetus has been the development of two-dimensional infrared photon echo (2D-IR) spectroscopy that represents a direct experimental probe of spectral diffusion as measured by the frequency-frequency time correlation function (FFCF). In isotopically dilute water, which is perhaps the most thoroughly studied system, the standard interpretation of the longest timescale observed in the FFCF is that it is associated with hydrogen-bond exchange dynamics. Here, we investigate this connection by detailed analysis of both the spectral diffusion timescales and their associated activation energies. The latter are obtained from the recently developed fluctuation theory for dynamics approach. The results show that the longest timescale of spectral diffusion obtained by the typical analysis used cannot be directly associated with hydrogen-bond exchanges. The hydrogen-bond exchange time does appear in the decay of the water FFCF, but only as an additional, small-amplitude ($< 3\%$) timescale. The dominant contribution to the long-time spectral diffusion dynamics is considerably shorter than the hydrogen-bond exchange time and exhibits a significantly smaller activation energy. It thus arises from hydrogen-bond rearrangements that occur in between successful hydrogen-bond partner exchanges, and particularly from hydrogen-bonds that transiently break before returning to the same acceptor.

I. INTRODUCTION

The development of two-dimensional infrared photon-echo (2D-IR) spectroscopy has driven considerable interest in spectral dynamics in liquids and other condensed phase environments.[1–4] This technique provides a method to monitor the fluctuations of a particular vibrational frequency, the spectral diffusion, to gain new insight into the liquid dynamics. This spectral diffusion is described by the frequency-frequency correlation function (FFCF) that represents a quantitative measure of the timescale(s) with which a vibrational mode loses memory of its frequency.

While 2D-IR spectroscopy has been applied across a diverse set of systems, liquid water is perhaps the best studied case. The water OH stretch vibration is of particular interest, because its frequency sensitively depends on the hydrogen-bond (H-bond) strength. The FFCF obtained by 2D-IR spectroscopy thus provides a unique probe of the H-bond fluctuation dynamics in the liquid. Several theoretical and simulation studies[5–11] have investigated the molecular origin of the OH frequency dephasing in liquid water, and led to a consensus about the role of H-bond rearrangements. However, different suggestions were made regarding the exact nature of these rearrangements and their short-ranged or collective character.

After these pioneering studies of frequency dephasing in water, it was shown[12,13] that a major contribution to H-bond rearrangements originates from H-bond exchanges, where a water OH group switches H-bond acceptors *via* a sudden angular "jump" of the OH bond. The extended jump model[12,13] (EJM) combines this jump mechanism with the slower tumbling of the intact H-bond between these jumps and is able to accurately predict not only the timescales of water OH reorientation,[12,13] but also the associated activation energies.[14] Additionally, direct evidence of these large-angle jumps in salt solutions was provided by polarization-sensitive 2D-IR spectroscopy measurements.[15]

These large-angle jumps occurring with H-bond exchanges represent the main underlying molecular step for much of the dynamics of water, including reorientation,[12,13] diffusion,[14,16–18] and shear viscosity.[16,19] Prior studies[8,9,20] have suggested that H-bond exchanges are also the cause of spectral diffusion, but others have proposed alternative interpretations.[10,11,21–24]

In this Paper, we carry out a detailed analysis of the FFCF for isotopically dilute liquid water (HOD in D_2O) with the aim of elucidating the dynamics to which it is sensitive. The particular focus is on how H-bond exchange dynamics appears in the spectral diffusion. In addition to the FFCF itself, we investigate its temperature derivative and hence the activation energies associated with the spectral diffusion timescales. This is accomplished by application of the recently developed fluctuation theory for dynamics.[14,18,19,25–31]

Before proceeding, we first note that the FFCF exhibits short-time (< 0.5 ps) dynamics, which appears to now be uniformly recognized as associated with underdamped, librational dynamics within the intact H-bond.[5–7,10,11,32] The focus of the present work, however, is the longer-time (picosecond) spectral diffusion that has been the subject of many studies and for which several interpretations have been proposed. While all studies

[a)] Electronic mail: damien.laage@ens.psl.eu
[b)] Electronic mail: wthompson@ku.edu

concur that this timescale reports on water H-bond rearrangement dynamics, it is important to note that the language used to describe the phenomena underlying spectral diffusion dynamics is not unambiguous. Namely, "H-bond dynamics" can encompass multiple physically distinct processes with increasing timescales: 1) the rearrangement of the H-bond geometry without breaking the H-bond itself, 2) transient breaking of H-bonds that occurs before another H-bond partner is found in an exchange event or that occurs without any exchange at all when an OH returns to its original H-bond acceptor, and 3) H-bond jumps in which the OH group switches from one acceptor to another. All three types of dynamics surely play some role in spectral diffusion and in the following we will attempt to carefully distinguish between them in our discussion.

We first provide a brief overview of the prior studies of water frequency dephasing and their interpretations. In explaining some of the earliest measurements of spectral diffusion, the relationship between the H-bond, O$\cdots$O, distance and the OH frequency was often invoked, and OH frequency dephasing was attributed to the overdamped O$\cdots$O bond relaxation caused by the large surrounding solvent friction.[21–23,33,34]

However, four subsequent parallel studies all found that spectral diffusion in water is not associated with modulation of the H-bond distance but rather with H-bond rearrangement dynamics.

First, Rey, Møller, and Hynes[5,7] showed that the O$\cdots$O vibration is underdamped and that the relationship between the OH frequency and this H-bond distance involves considerable dispersion, notably due to the librational motion. By contrasting the frequency dynamics of all water OH groups and that of OH groups engaged in intact H-bonds, they concluded that "...the one-to-one frequency-H-bond length assumption is not valid and that the observed experimental time scale should be interpreted in terms of H-bond-breaking and -making dynamics."[5] This picture sat in contrast to the previous descriptions centered on the H-bond distance alone and stressed the importance of H-bond rearrangement dynamics.

In concurrent work, Lawrence and Skinner[8,9] simulated both the spectral diffusion and H-bond dynamics and also concluded that "at longer times the decay of the spectral diffusion TCF is due to hydrogen bond breaking and making dynamics."[8] More specifically, they proposed that the spectral diffusion time, τ_ω, is equal to the total rate constant for achieving equilibrium *via* both forward and backward H-bond exchanges. Using the intermittent H-bond lifetime, $\tau_{\rm HB}$, as a proxy for the H-bond exchange time, τ_0, they argued then the spectral diffusion time is given by $\tau_\omega = \tau_{\rm HB}/2$. There are, however, at least two unresolved puzzles associated with this viewpoint. First, subsequent characterization of H-bond exchanges *via* the jump mechanism[12,13] led to an improved determination of the H-bond exchange time from simulations as $\tau_0 \simeq 3.1 - 3.7$ ps.[14,35,36] This value is thus significantly longer than the H-bond dynamics considered in Ref. 8, and more than twice slower than the spectral diffusion time of isotopically dilute HOD in D_2O determined in both simulations and measurements to be $\tau_\omega \simeq 1 - 1.5$ ps.[2,10,37,38] H-bond exchanges are thus too slow to explain the fast frequency dephasing. Second, this would require spectral diffusion to be mostly caused by specific H-bond rearrangements that are only accomplished by an exchange of H-bond partners, even though both initial and final partners are water molecules with identical average properties. The nature of these rearrangements would need to be characterized.

A third contribution by Fecko *et al.*[10] stressed the collective character of the H-bond rearrangements causing the spectral dephasing. They compared the FFCF to the time correlation functions of different contributions to the OH frequency (within a perturbation theory description) and some of the geometric parameters (O$\cdots$O distance and tetrahedrality parameter, q) and found they all have similar long-time decays. Thus, they concluded that the spectral diffusion "...reflects a variety of relaxation mechanisms, including collective rearrangement of the hydrogen-bond network, as well as density and polarization fields, on length scales greater than a molecular diameter." They further argue that these longer time dynamics, which do include the "...breaking and forming of hydrogen bonds, involve the concerted motions of many molecules."

Finally, a different interpretation was later proposed by Garrett-Roe and Hamm[11] who examined the spectral diffusion dynamics based on MD simulations using the SPC model within a perturbation theory approach. Their analysis was based on the calculation of three-time FFCFs rather than the usual (two-time) measure of spectral dynamics and they found that their results "...show that hydrogen bond rearrangements occur largely perpendicular to the OH stretch frequency axis..." However, the motions causing the OH frequency dephasing were not discussed.

In the remainder of this paper, we examine the spectral diffusion and H-bond exchange dynamics for HOD in D_2O to gain greater insight into their connection. These analyses indicate that the spectral diffusion timescale, as it is typically extracted from the long-time decay of the FFCF, is not consistent with that of an H-bond exchange. Rather, we offer evidence that the H-bond jump timescale *is* present in the FFCF decay, but only as an additional, small-amplitude timescale.

II. THEORY

Spectral diffusion is most clearly quantified in terms of the normalized frequency-frequency time correlation function (FFCF) given by

$$C_\omega(t) = \frac{\langle \delta\omega_{01}(0)\delta\omega_{01}(t)\rangle}{\langle \delta\omega_{01}^2\rangle}, \qquad (1)$$

where $\delta\omega_{01}(t) = \omega_{01}(t) - \langle\omega_{01}\rangle$ is the fluctuation in the transition frequency at time t and $\langle\cdots\rangle$ represents a thermal average. The spectral diffusion time, which we will refer to as τ_ω is typically extracted as either the longest timescale of a tri-exponential fit[2,38,39] of Eq. (1) or the timescale from a single exponential fit to $C_\omega(t)$ for long times, *e.g.*, $t > 1.5$ ps.[40] Note that the FFCF, under reasonable assumptions (at least for the neat liquid),[41] can be extracted from the center-line-slope of a 2D-IR spectrum and is thus experimentally accessible.

In the present analysis, we use a multi-exponential fit,

$$C_\omega(t) = \sum_\alpha A_\alpha e^{-k_\alpha t}, \tag{2}$$

to describe the FFCF. We consider fits with both three and four exponentials and in all cases the shortest three timescales, $\tau_\alpha = 1/k_\alpha$, are assigned as the inertial (τ_{iner}), librational (τ_{lib}), and spectral diffusion (τ_ω) times, respectively. When fitting to three and four exponentials we will denote the spectral diffusion time as $\tau_\omega^{(3)}$ and $\tau_\omega^{(4)}$, respectively. When four exponentials are used, the longest timescale will be the separately calculated jump time, τ_0. Note that the inertial and librational decays are not qualitatively exponential, but Eq. (2) provides an adequate description of the associated timescales without adversely affecting the longer timescales that are the focus of the present investigation.

The jump time characterizing H-bond exchanges can be obtained from the stable-states time correlation function,

$$C_{ab}(t) = \langle n_a(0)\, n_b(t)\rangle, \tag{3}$$

where here n_a (n_b) equals 1 for a given OH if it is H-bonded to acceptor a (b) and is 0 otherwise. Thus, for a given OH initially H-bonded to an acceptor we can denote as a, the contribution to C_{ab} at $t = 0$ is zero and it only changes to 1 when the OH has switched to a new acceptor (b). Thus, $C_{ab}(t)$ rises on a timescale equal to the rate constant for H-bond exchanges. Or, equivalently, $1 - C_{ab}(t)$ decays as an exponential with a timescale equal to the jump time. In practice, some short-time non-exponential dynamics is observed in $C_{ab}(t)$ and we fit it to a bi-exponential where the longer timescale is the jump time τ_0.

We calculate the activation energy for the spectral diffusion timescales based on the fluctuation theory for dynamics.[28] This approach directly evaluates the temperature derivative of a time correlation function from simulations at a single temperature. A detailed derivation can be found in Ref. 28. Briefly, for the FFCF in Eq. (1), the derivative with respect to $\beta = 1/k_bT$ is given by

$$\begin{aligned}\frac{\partial C_\omega(t)}{\partial\beta} &= -\frac{\langle\delta H(0)\,\delta\omega_{01}(0)\delta\,\omega_{01}(t)\rangle}{\langle\delta\omega_{01}^2\rangle} \\ &\quad + \frac{\langle\delta H(0)\,\delta\omega_{01}^2\rangle\,\langle\delta\omega_{01}(0)\delta\,\omega_{01}(t)\rangle}{\langle\delta\omega_{01}^2\rangle^2} \\ &= -C_{\omega,H}(t),\end{aligned} \tag{4}$$

where $\delta H(0) = H(0) - \langle H\rangle$ is the fluctuation in the total system energy. We have noted that T only appears in the Boltzmann weighting and normalizing canonical partition functions implicit in the thermal averages in $C_\omega(t)$. Note that the time-correlation functions in Eq. (4) can be evaluated at a single temperature using the same simulations from which $C_\omega(t)$ is obtained (see Sec. III A). They give the analytical derivative of the FFCF in contrast the numerical derivative obtained an Arrhenius analysis. The second term in Eq. (4) represents the temperature dependence of the FFCF normalization factor while the first correlates the spectral dynamics with $\delta H(0)$, the total energy in the system relative to its average value, *e.g.*, faster (slower) spectral diffusion when more (less) energy is available corresponds to a positive spectral diffusion activation energy.

The derivatives of the timescales are then obtained by fitting Eq. (4) to the derivative of the fitting function in Eq. (2),

$$\frac{\partial C_\omega(t)}{\partial\beta} = \sum_\alpha \left[\frac{\partial A_\alpha}{\partial\beta} - A_\alpha t\frac{\partial k_\alpha}{\partial\beta}\right] e^{-k_\alpha t}. \tag{5}$$

In fitting $\partial C_\omega(t)/\partial\beta$ the timescales and amplitudes obtained from the fit of $C_\omega(t)$ are used such that the fitting parameters are only $\partial A_\alpha/\partial\beta$ and $\partial k_\alpha/\partial\beta$. The activation energy associated with the α timescale is then given by

$$E_{a,\alpha} = -\frac{1}{k_\alpha}\frac{\partial k_\alpha}{\partial\beta}. \tag{6}$$

Note that in this approach the activation energy is evaluated from simulations at a single temperature (no Arrhenius analysis is involved).

In an analogous fashion, the derivative of the jump TCF, Eq. (3), can be obtained as[14,42]

$$\frac{\partial[1 - C_{ab}(t)]}{\partial\beta} = \langle\delta H(0)\, n_a(0)\, n_b(t)\rangle. \tag{7}$$

This derivative is also fit to the form in Eq. (5), but with only two timescales. The jump time activation energy, $E_{a,0}$, is then given by Eq. (6) for the longer, jump, timescale τ_0.

III. COMPUTATIONAL METHODS

A. Simulation Details

The simulations were carried out using the Large-scale Atomic/Molecular Massively Parallel Simulator (LAMMPS).[43] A cubic, fully periodic, simulation cell with side lengths of 21.725311 Å was filled with 343 water molecules described by the SPC/E model,[44] giving a density of 1.00 g/cm^3. A simulation timestep of 1 fs was used. The Particle-Particle-Particle Mesh Ewald summation method was used to calculate electrostatic interactions, with a tolerance parameter of 1×10^{-4}.[45,46] Water

bonds and angles were held rigid using the SHAKE algorithm with a tolerance parameter of 1×10^{-4}.[47]

One 200 ns NVT trajectory was propagated at 298.15 K, with positions and momenta saved every 1 ps, yielding 200,000 configurations. Initial velocities were selected from a Maxwell-Boltzmann distribution. The initial configuration was generated using PACKMOL. The Nosé-Hoover thermostat damping parameter was 100 fs.[48,49]

From each saved configuration, a 20 ps NVE simulation was run from which time correlation functions were calculated. Configurations from each simulation were saved every 10 fs, giving 2000 total configurations per NVE trajectory. Reported TCFs are calculated as the average across the set of NVE trajectories and derivatives are calculated by weighting by the energy fluctuation of each trajectory according to Eqs. (4) and (7). All fits of TCFs were calculated using the Levenberg-Marquardt algorithm.[50,51] All uncertainties are reported as a 95% confidence interval according to the Student's t-distribution over an average of ten blocks (each block representing 20,000 configurations).[52]

We have repeated the above analysis at room temperature for two other water models developed by Skinner and co-workers, the E3B2 and the E3B3 water models.[53,54] These models explicitly add 3-body effects on top of existing force fields (TIP4P for E3B2 and TIP4P/2005 for E3B3). In general, the simulation details remain the same as above; however, for the E3B2 and E3B3 models the side lengths were 21.7710 and 21.7799 Å, respectively.

B. Vibrational Frequencies

The OH vibrational transition frequencies are related to the electric field imposed on the H atom by the water molecules surrounding them, as described by the empirical mapping approach developed by Corcelli, Skinner, and co-workers.[55–58] In this work, we use maps that have been previously developed for the SPC/E, TIP4P, and TIP4P/2005 force fields.[57,58] In previous work, Skinner and co-workers have used the TIP4P map in calculations of the FFCF using the E3B2 and E3B3 models. Each of these maps takes the electric field experienced by each hydrogen atom from waters within 7.831 Å of the H atom, which can be written as

$$\mathcal{E}_i(t) = \vec{e}_{OH,i}(t) \cdot \vec{\mathcal{E}}(\vec{r}_{H,i}, t), \tag{8}$$

and correlates it to the transition frequency obtained from density functional theory calculations. In the above expression, the electric field is calculated in atomic units, $\vec{r}_{H,i}$ is the position of the i^{th} H atom, and $\vec{e}_{OH,i}$ is a unit vector pointing along the OH bond.

For SPC/E, the transition frequency $\omega^i_{01}(t)$, in cm^{-1}, of the ith OH at time t can be written as

$$\omega^i_{01}(t) = 3761.6 - 5060.4\,\mathcal{E}_i(t) - 86225\,\mathcal{E}_i(t)^2. \tag{9}$$

Similarly, the TIP4P map (used for both E3B2 and E3B3) is,

$$\omega^i_{01}(t) = 3760.2 - 3541.7\,\mathcal{E}_i(t) - 152677\,\mathcal{E}_i(t)^2. \tag{10}$$

The density functional theory calculations used to obtain these "maps" are obtained from quantum-mechanical/point charge cluster calculations using configurations selected from MD simulations. The one-dimensional OH potential is calculated and the corresponding vibrational Schrödinger equation is solved to obtain the frequency.[57,58]

IV. RESULTS AND DISCUSSION

A. Spectral Diffusion Timescales

We begin by considering the spectral diffusion dynamics as described by the FFCF. We have calculated the FFCF for three different water models and the timescales and amplitudes for all the simulations are given in Table I. We first discuss the results for SPC/E water at 298.15 K, which are shown in Fig. 1. The fit to a tri-exponential function, Eq. (2), is also shown, which gives inertial and librational timescales of 33 and 374 fs, respectively, and a spectral diffusion time of $\tau_\omega^{(3)} = 1.30 \pm 0.03$ ps. This last value is consistent with previous simulation studies[2,39,59–61] for SPC/E water that found 0.9,[60] 0.98,[39] and 1.2 ps.[61] Similarly, photon-echo and 2D-IR measurements have found this timescale to be 0.9, 1.2, or 1.4 ps for HOD/D_2O and 1.7–1.8 ps for HOD/H_2O.[2,10,38,39,62]

However, it is evident from examination of the FFCF shown on a semi-log scale in the inset of Fig. 1 that this

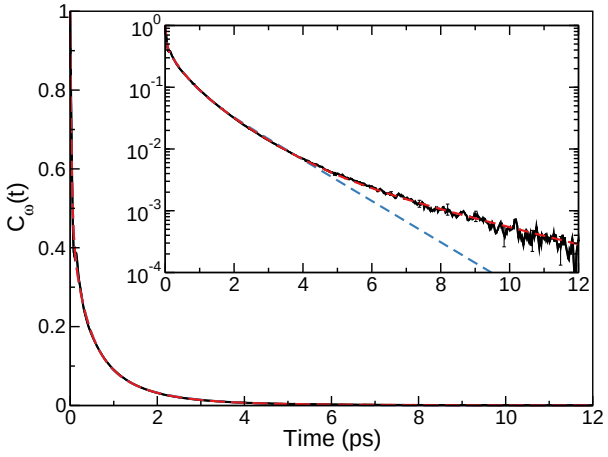

FIG. 1: The room temperature frequency-frequency correlation function (black solid line) for SPC/E water is shown along with fits using three (blue dashed line) and four (red dashed line) exponentials. Inset: Semi-log plot.

3-Exponential Parameters								
Model	T (K)	τ_{iner}	τ_{lib}	$\tau_\omega^{(3)}$		A_{iner}	A_{lib}	$A_\omega^{(3)}$
SPC/E	298.15	0.033_1	0.374_9	1.30_3		0.540_2	0.316_5	0.145_7
E3B2	298.15	0.033_1	0.482_7	2.14_4		0.547_2	0.324_3	0.129_4
E3B3	298.15	0.030_1	0.489_3	2.27_2		0.588_1	0.308_1	0.104_1
4-Exponential Parameters									
Model	T (K)	τ_{iner}	τ_{lib}	$\tau_\omega^{(4)}$	τ_0	A_{iner}	A_{lib}	$A_\omega^{(4)}$	A_{τ_0}
SPC/E	298.15	0.033_1	0.320_4	0.98_2	3.16_1	0.532_2	0.266_4	0.190_4	0.013_1
E3B2	298.15	0.031_1	0.330_5	1.20_2	4.59_1	0.524_2	0.241_3	0.209_3	0.026_1
E3B3	298.15	0.029_1	0.357_3	1.19_2	4.30_1	0.572_1	0.233_3	0.168_3	0.027_1

TABLE I: Timescales (in ps) and amplitudes of the FFCF calculated from three- (top) and four- (bottom) exponential fits. Subscripts represent uncertainty in the trailing digit(s).

tri-exponential description is not accurate at times longer than 4 ps. Rather, the data indicate that an additional timescale is present in the dynamics. Based on the hypothesis that these slower dynamics were in fact those associated with the exchange of H-bond acceptors, we also fit the FFCF with Eq. (2) using four exponentials with the longest timescale constrained to the jump time. The jump time was separately calculated as described in Sec. II from the same simulations and found to be $\tau_0 = 3.16 \pm 0.01$ ps. (We use a strict geometric definition of the H-bond as $R_{O_d \cdots O_a} \leq 3.1$ Å, $r_{H \cdots O_a} \leq 2.0$ Å, and $\theta_{H-O_d \cdots O_a} \leq 20°$, where "$d$" indicates donor and "$a$" acceptor.) This four-exponential fit is shown in Fig. 1 and provides an excellent description of the full decay of the FFCF (out to 12 ps where the FFCF is less than 0.001). This indicates that H-bond exchanges, *i.e.*, jumps, are indeed present in the FFCF, but only as a long time component described by the jump time and with an amplitude we find to be 1.3% for the SPC/E model. In contrast, the third timescale, $\tau_\omega^{(4)}$, has an amplitude of 19.0%.

The tri-exponential fit yields a longest timescale, $\tau_\omega^{(3)}$, that represents a mixture of the more rapid spectral diffusion dynamics in between exchanges of H-bond acceptors and that directly associated with H-bond exchanges as described by τ_0. The mixture is not an even one and the dominant component is that which does not involve H-bond jumps. Because the jump time enters with only a small amplitude, the spectral diffusion timescale is only modestly different in the two descriptions with $\tau_\omega^{(4)} = 0.98 \pm 0.01$ ps. Notably, these results indicate that if one only calculates, measures, or fits the FFCF to times less than $\sim 4-5$ ps, the resulting timescale is not significantly related to H-bond exchanges. An f-test, with a 95% confidence interval, confirms that the 4-exponential fitting function provides a statistically significant improvement in the description of the FFCF over the 3-exponential function.[63]

It is important to evaluate the generality of this result by considering other water models. To this end, we have carried out the same calculation of the FFCF for the E3B2[53] and E3B3[54] water models, which add three-body interactions to fixed charge models as noted in Sec. III A. The former has been previously used to investigate water spectral diffusion and its temperature dependence.[40] The FFCFs obtained with these models are shown in Fig. 2 and the parameters obtained from fitting them are provided in Table I.

The spectral diffusion dynamics for these E3B force fields are qualitatively the same as that observed for

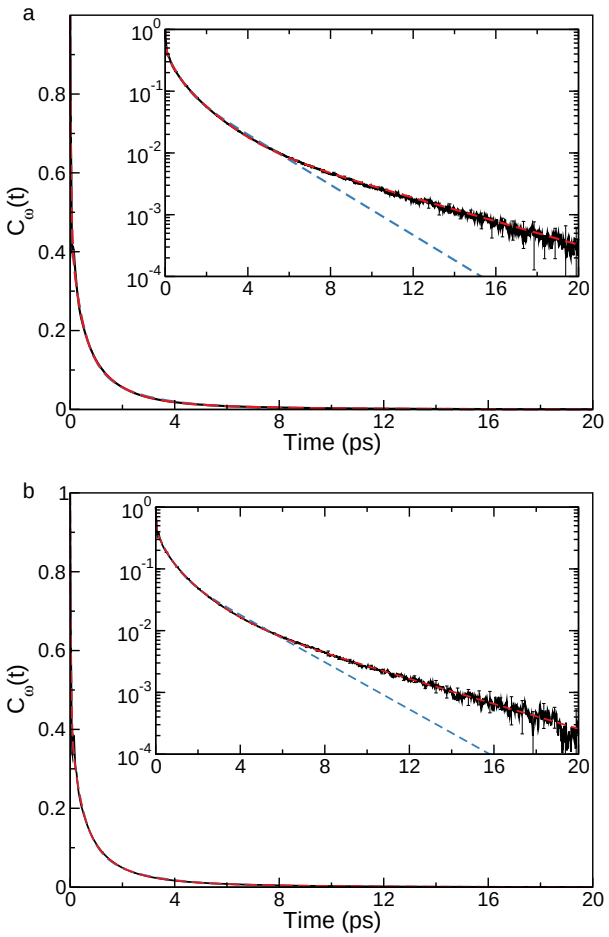

FIG. 2: Same as Fig. 1, but for the (a) E3B2 and (b) E3B3 water models.

SPC/E water in Fig. 1. Namely, a tri-exponential fit is consistent with the calculated FFCF only for shorter times, here less than 6 ps. At times longer than this the FFCF decays more slowly than represented by the spectral diffusion time obtained in the fit, $\tau_\omega^{(3)} = 2.1 - 2.3$ ps; see Table I. These times are consistent with the ~ 2 ps previously reported by Ni and Skinner for the E3B2 model.[40] This is quantitatively slower than that obtained for the SPC/E model, which represents the primary difference between the descriptions. Because of this behavior, we are able to resolve the FFCF for the E3B models out to longer times than that for SPC/E water.

As with the SPC/E description, these $\tau_\omega^{(3)}$ spectral diffusion times are considerably shorter than the calculated jump times, which are also given in Table I. The jump times of $\tau_0 = 4.59$ and 4.30 ps for E3B2 and E3B3, respectively, are significantly larger than the SPC/E value. Using these values as the timescale for an added fourth exponential in fitting $C_\omega(t)$ gives excellent agreement over the full time range. However, this jump time contribution to the FFCF is still small, with an amplitude of $2.6 - 2.7\%$ compared to the faster spectral diffusion time amplitude of $21 - 17\%$. We also note that the addition of this jump time component dramatically reduces the spectral diffusion time obtained to 1.2 ps for both E3B models.

Thus, for all three water models we find the same features in the FFCF that indicate a small role, $< 3\%$ of the total response, for H-bond exchanges that occurs on timescales longer than the dominant component of $1 - 1.2$ ps. The latter occurs more rapidly than H-bond exchanges, indicating it has a different physical origin.

B. Activation Energies

To further explore the role of H-bond exchanges in the spectral diffusion dynamics, we now turn to an examination of the activation energies of the timescales involved. These activation energies can shed light on the mechanistic origins of the decay times present in the FFCF. Most importantly, if the spectral diffusion time is associated with H-bond exchanges, it should exhibit the same activation energy as the jump time.[64] Deviations from this prediction are indicative of a different mechanistic origin (or origins) of the spectral diffusion timescale.

We evaluate this directly by calculating the temperature-, or more precisely, the β-derivative of the full FFCF as described in Sec. II and expressed in Eq. (4). The results are shown in Fig. 3 for all three water models along with the fits to the form given in Eq. (5). As with the FFCF itself, it is clear that $\partial C_\omega(t)/\partial\beta$ is not adequately described at long times by the three-exponential fit, but the agreement is excellent when a small additional component with a timescale equal to the jump time, τ_0, is included.

As noted in Sec. II, the activation energy of each timescale can be obtained from fitting the derivative

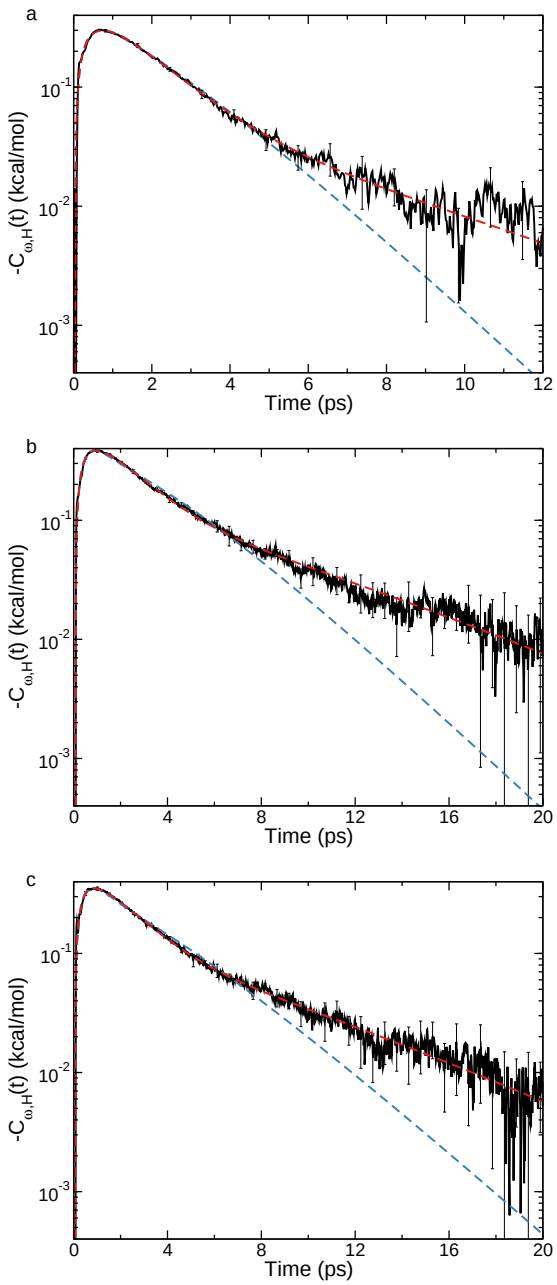

FIG. 3: The β derivative of the FFCF, $\partial C_\omega(t)/\partial\beta$, versus time (black solid line) is shown for the (a) SPC/E, (b) E3B2, and (c) E3B3 water models with three- (blue dashed line) and four- (red dashed line) exponential fits, Eq. (5). In the latter, the longest timescale is fixed as the jump time, τ_0.

FFCF, $C_{\omega,H}(t)$. The results of this analysis are given in Table II. (Note that the four-exponential fits shown in Fig. 3 use the jump time τ_0 *and* its derivative $\partial\tau_0/\partial\beta$, both of which are obtained from a separate analysis of the trajectories.) The calculated activation energies for the spectral diffusion time are not the same as that for the jump time, independent of whether the three- or four-

SPC/E Water Model				
Timescale	E_a	KE	LJ	$Coul$
τ_0	3.30_3	0.95_1	-0.88_4	3.23_6
$\tau_\omega^{(3)}$	2.24_{51}	0.51_{20}	-0.60_{50}	2.33_{98}
$\tau_\omega^{(4)}$	1.68_{98}	0.41_{34}	-0.94_{69}	$2.20_{1.48}$
E3B2 Water Model				
Timescale	E_a	KE	LJ	$Coul$
τ_0	4.43_2	1.10_2	-1.16_2	4.49_2
$\tau_\omega^{(3)}$	3.36_{15}	0.83_{16}	-0.91_{15}	3.45_{36}
$\tau_\omega^{(4)}$	2.49_{20}	0.51_{14}	-0.78_{20}	2.76_{42}
E3B3 Water Model				
Timescale	E_a	KE	LJ	$Coul$
τ_0	4.14_3	1.06_1	-1.37_3	4.45_4
$\tau_\omega^{(3)}$	2.81_{35}	0.76_9	-0.94_{17}	2.98_{36}
$\tau_\omega^{(4)}$	2.55_{30}	0.53_{10}	-1.13_{30}	3.15_{40}

TABLE II: Activation energies and kinetic (KE), Lennard-Jones (LJ), and Coulombic ($Coul$) energy components for the jump time τ_0 and the spectral diffusion times obtained from three-, $\tau_\omega^{(3)}$, and four-, $\tau_\omega^{(4)}$, exponential fits of the derivative FFCF, $C_{\omega,H}(t)$. All energies are in kcal/mol; subscripts represent uncertainty in the trailing digit(s).

exponential fit is considered. Specifically, the jump time has a significantly higher E_a compared to the spectral diffusion time. This difference is increased when the long-time behavior is more accurately described by inclusion of the fourth exponential with timescale τ_0. This indicates that the spectral diffusion times are determined by a process with a lower effective barrier than that for H-bond exchanges. Consistent with our analysis of the FFCF, this suggests that the spectral diffusion time cannot be solely, or even primarily, associated with H-bond jumps. Furthermore, as was the case for the FFCF, an f-test with 95% confidence intervals confirms that the derivative 4-exponential fitting function provides a statistically significant improvement over the 3-exponential derivative function.[63] Importantly, this demonstrates that the explicit inclusion of the jump activation energy in this fit improves the quality of the fit of the long-time behavior of the FFCF.

Ni and Skinner previously reported a spectral diffusion activation energy of 3.85 kcal/mol for the E3B2 water model from an Arrhenius analysis.[40] This is most directly comparable to E_a for $\tau_\omega^{(3)}$ in the present calculations, for which we obtain 3.36 ± 0.15 kcal/mol. It is not clear if the two results are statistically different, however, as in Ref. 40 they obtain the timescale from fitting the FFCF for times longer than 1.5 ps to a single exponential and use a wide temperature range ($283 - 363$ K) for the Arrhenius analysis.[65] It is important to note that while these values are similar to activation energies reported for the spectral diffusion time from measurements – values of 3.4 ± 0.5 kcal/mol[66,67] and 3.5 ± 0.2 kcal/mol[68] have been reported (though Perakis and Hamm argue that 6.2 ± 0.2 kcal/mol, taken under different polarization conditions, is a better estimate[68]) – they are not in agreement with the jump time activation energy obtained from the same water model, $E_{a,0} = 4.43 \pm 0.02$ kcal/mol. Thus our present results indicate that the spectral diffusion activation energy is *not* the same as the jump activation energy, and thus it is not associated with H-bond exchanges.

C. Mechanistic Insight

The fluctuation theory approach provides a rigorous way to decompose the activation energy into contributions from different components of the total energy by recognizing that $\delta H(0) = \delta KE(0) + \delta U_{LJ}(0) + \delta U_{Coul}(0)$, where $\delta KE(0)$, $\delta U_{LJ}(0)$, and $\delta U_{Coul}(0)$ are the kinetic, Lennard-Jones, and Coulombic energy fluctuations, respectively. This sum can be used to replace $\delta H(0)$ in Eqs. (4) and (7) to yield three separate derivative time correlation functions, each of which can then be fit with Eq. (5) to extract the activation energy contributions associated with each term. These contributions can be interpreted based on Tolman's perspective.[69] Tolman showed that for a chemical reaction, the activation energy can be rigorously written as $E_a = \langle H \rangle_{reacting} - \langle H \rangle_{reactants}$, *i.e.*, the average energy of the species that react minus the average energy of reactants. In this context, the Lennard-Jones contribution to the activation energy is $E_{a,LJ} = \langle U_{LJ} \rangle_{reacting} - \langle U_{LJ} \rangle_{reactants}$ or the average Lennard-Jones energy of reacting species minus the average Lennard-Jones energy of reactants. Thus, such decompositions provide otherwise unavailable mechanistic insight into how different kinds of energy in the system promote or inhibit the process of interest.

The decomposition of the FFCF derivative, $\partial C_\omega(t)/\partial\beta$, into its kinetic, Lennard-Jones, and Coulombic contributions is shown in Fig. 4 for SPC/E water. The activation energy components obtained from the fitting are given in Table II, where E3B2 and E3B3 results are also listed. Consistent with what we have previously found for the activation energies for OH reorientation,[18,27] diffusion,[18,30] viscosity,[19] and H-bond jumps of water,[14] the Coulombic interactions represent the dominant contribution, though they are in competition with the smaller Lennard-Jones component. Indeed, $E_{a,Coul}$ is nearly equal to the total activation energy for the spectral diffusion timescale if a three-exponential fit is used and larger than it in the four-exponential fitting. On the other hand, $E_{a,LJ}$ is negative, reflecting the natural tension between the Coulombic and Lennard-Jones interactions in an H-bond. However, the Lennard-Jones contribution is significantly smaller than $E_{a,Coul}$, as is the positive kinetic energy component.

The decomposition of the activation energies for the SPC/E model are suggestive of differences between the results for the H-bond jump and spectral diffusion times. However, the comparatively large statistical

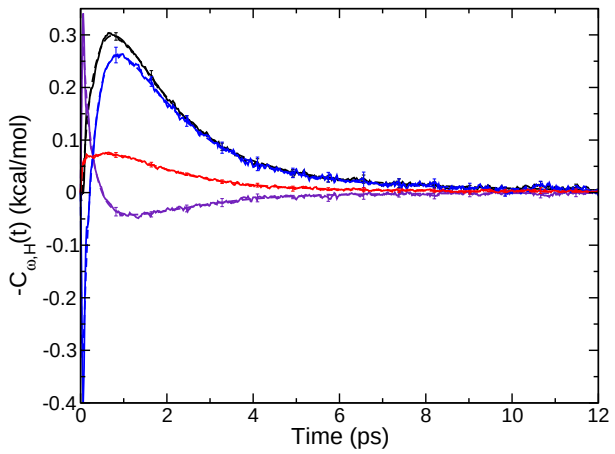

FIG. 4: The β derivative of the FFCF, $\partial C_\omega(t)/\partial\beta$, versus time (black solid line) and its kinetic (red solid line), Lennard-Jones (violet solid line), and Coulombic (blue solid line) energy contributions for the SPC/E water model. Four-exponential fits, Eq. (5), are also shown (dashed lines of the same color; not easily visible because of the high quality of the fit.)

uncertainties do not allow them to be distinguished except for the total activation energy and the kinetic energy component; these are both higher for the jump time than the spectral diffusion result. For the E3B models, the errors are smaller (particularly for the $\tau_\omega^{(4)}$ timescale due to its larger amplitude) and it is then clear that the differences observed in the total jump and spectral diffusion activation energies are also present in the kinetic, Lennard-Jones, and Coulombic components. In all cases, the jump time has components that are larger in absolute value compared to the spectral diffusion results (independent of the fitting method). This is suggestive of weaker energetic barriers for spectral diffusion compared to H-bond exchanges.

V. CONCLUSIONS

We have examined the connection between spectral diffusion and H-bond exchange dynamics in three water models by calculating and analyzing the frequency-frequency correlation function for the OH vibration of an HOD in D_2O. We find that the long-time decay of this FFCF is not adequately described by a single spectral diffusion timescale. However, inclusion of an additional decay component with a timescale equal to the H-bond exchange time, τ_0, yields an excellent fit of the calculated FFCF. This exchange time component has a small amplitude ($< 3\%$) and is thus a minor component of the spectral diffusion dynamics. The remaining spectral diffusion timescale is found to be $\sim 1 - 1.2$ ps, consistent with experimental measurements,[10,38] but significantly faster than the H-bond exchange time.

We have also used dynamical fluctuation theory to calculate and compare the spectral diffusion and H-bond jump activation energies from the temperature (or β) derivative of the FFCF. This derivative time correlation function is also only well described when a small-amplitude decay based on the H-bond jump time is included. Moreover, the resulting activation energies are different for the spectral diffusion time and the H-bond jump time. The same is true for the components of the two activation energies (available within the fluctuation theory) associated with kinetic, Coulombic, and Lennard-Jones energies in the system.

The results show that the spectral diffusion time is shorter than that for H-bond exchanges and it has a smaller activation energy. Thus, it clearly corresponds to processes that happen in between H-bond exchanges and require less energy than that necessary to fully break one H-bond and form another. This implicates rearrangements of the H-bond structure within the intact H-bond and transient breaking of H-bonds (in which the OH returns to its original H-bond acceptor) as the motions associated with the spectral diffusion time. While H-bond exchanges also contribute to the spectral diffusion, they do so at longer times and with a comparatively small amplitude.

This minor contribution of H-bond jumps to the spectral diffusion is consistent with a picture in which only jumps between acceptors that yield different H-bonding structures are expected to lead to a difference in the equilibrium OH frequency. While this is the case in aqueous solutions containing different types of H-bond acceptors,[70,71] in neat liquid water most of the frequency dephasing can be accomplished by rearrangements of the H-bonding arrangement either without breaking the original H-bond (through motions of the surrounding waters) or by transiently breaking and reforming the H-bond with the original acceptor. These motions occur on a picosecond timescale, more than three times faster than that for H-bond exchanges.

ACKNOWLEDGMENTS

The authors would like to thank Professor Brian B. Laird for many useful discussions. This work was supported by the National Science Foundation under Grant No. CHE-1800559. This material is based on the work supported by the National Science Foundation Graduate Research Fellowship under Grant Nos. 1540502 and 1451148 as well as the National Science Graduate Research Opportunities Worldwide Program. The calculations were performed at the University of Kansas Center for Research Computing (CRC).

DATA AVAILABILITY

The data that support the findings of this study are available from the corresponding author upon reasonable request.

[1] M. D. Fayer, "Dynamics of liquids, molecules, and proteins measured with ultrafast 2D IR vibrational echo chemical exchange spectroscopy," Annu. Rev. Phys. Chem. **60**, 21–38 (2009).

[2] H. J. Bakker and J. L. Skinner, "Vibrational spectroscopy as a probe of structure and dynamics in liquid water," Chem. Rev. **110**, 1498–1517 (2010).

[3] P. Hamm and M. Zanni, *Concepts and methods of 2D infrared spectroscopy* (Cambridge Univ Press, Cambridge, UK, 2011).

[4] T. Elsaesser, "Two-dimensional infrared spectroscopy of intermolecular hydrogen bonds in the condensed phase." Acc Chem Res **42**, 12201228 (2009).

[5] R. Rey, K. B. Møller, and J. T. Hynes, "Hydrogen bond dynamics in water and ultrafast infrared spectroscopy," J. Phys. Chem. A **106**, 11993–11996 (2002).

[6] R. Rey, K. B. Møller, and J. T. Hynes, "Ultrafast vibrational population dynamics of water and related systems: A theoretical perspective," Chem. Rev. **104**, 1915–1928 (2004).

[7] K. B. Møller, R. Rey, and J. T. Hynes, "Hydrogen bond dynamics in water and ultrafast infrared spectroscopy: A theoretical study," J. Phys. Chem. A **108**, 1275–1289 (2004).

[8] C. P. Lawrence and J. L. Skinner, "Ultrafast infrared spectroscopy probes hydrogen-bonding dynamics in liquid water," Chem. Phys. Lett. **369**, 472–477 (2003).

[9] C. P. Lawrence and J. L. Skinner, "Vibrational spectroscopy of HOD in liquid D_2O. III. Spectral diffusion, and hydrogen-bonding and rotational dynamics," J. Chem. Phys. **118**, 264 (2003).

[10] C. J. Fecko, J. D. Eaves, J. J. Loparo, A. Tokmakoff, and P. L. Geissler, "Ultrafast hydrogen-bond dynamics in the infrared spectroscopy of water." Science **301**, 1698–1702 (2003).

[11] S. Garrett-Roe and P. Hamm, "Three-point frequency fluctuation correlation functions of the OH stretch in liquid water," J. Chem. Phys. **128**, 104507 (2008).

[12] D. Laage and J. T. Hynes, "A molecular jump mechanism of water reorientation," Science **311**, 832–835 (2006).

[13] D. Laage and J. T. Hynes, "On the molecular mechanism of water reorientation." J. Phys. Chem. B **112**, 14230–14242 (2008).

[14] Z. A. Piskulich, D. Laage, and W. H. Thompson, "Activation energies and the extended jump model : How temperature affects reorientation and hydrogen-bond exchange dynamics in water ," The Journal of Chemical Physics **074110**, 074110 (2020).

[15] M. Ji, M. Odelius, and K. J. Gaffney, "Large angular jump mechanism observed for hydrogen bond exchange in aqueous perchlorate solution," Science **328**, 1003–1005 (2010).

[16] S. Glasstone, L. K.J., and H. Eyring, *The Theory of Rate Processes*, edited by McGraw-Hill (New York, 1941).

[17] S. Shimizu and N. Matubayasi, "Ion hydration: Linking self-diffusion and reorientational motion to water structure," Phys. Chem. Chem. Phys. **20**, 5909–5917 (2018).

[18] Z. A. Piskulich, O. O. Mesele, and W. H. Thompson, "Removing the barrier to the calculation of activation energies: Diffusion coefficients and reorientation times in liquid water," J. Chem. Phys. **147**, 134103 (2017).

[19] C. Mendis, Z. A. Piskulich, and W. H. Thompson, "Tests of the Stokes-Einstein relation through the shear viscosity activation energy of water," J. Phys. Chem. B. **123**, 5857–5865 (2019).

[20] P. L. Kramer, J. Nishida, C. H. Giammanco, A. Tamimi, and M. D. Fayer, "Observation and theory of reorientation-induced spectral diffusion in polarization-selective 2d ir spectroscopy." J. Chem. Phys. **142**, 184505 (2015).

[21] R. Laenen, C. Rauscher, and A. Laubereau, "Dynamics of local substructures in water observed by ultrafast infrared hole burning," Phys Rev Lett **80**, 2622 (1998).

[22] S. Woutersen and H. J. Bakker, "Hydrogen bond in liquid water as a brownian oscillator," Phys Rev Lett **83**, 2077 (1999).

[23] H. J. Bakker, H.-K. Nienhuys, G. Gallot, N. Lascoux, G. M. Gale, J.-C. Leicknam, and S. Bratos, "Transient absorption of vibrationally excited water," J. Chem. Phys. **116**, 2592 (2002).

[24] D. Laage, G. Stirnemann, F. Sterpone, and J. T. Hynes, "Water jump reorientation: from theoretical prediction to experimental observation." Acc Chem Res **45**, 5362 (2012).

[25] O. O. Mesele and W. H. Thompson, "Removing the barrier to the calculation of activation energies," J. Chem. Phys. **145**, 13410 (2016).

[26] Z. A. Piskulich, O. O. Mesele, and W. H. Thompson, "Expanding the calculation of activation volumes: Self-diffusion in liquid water," J. Chem. Phys. **148**, 134105 (2018).

[27] Z. A. Piskulich and W. H. Thompson, "The activation energy for water reorientation differs between IR pump-probe and NMR measurements," J. Chem. Phys. **149**, 164504 (2018).

[28] Z. A. Piskulich, O. O. Mesele, and W. H. Thompson, "Activation energies and beyond," The Journal of Physical Chemistry A **123**, 7185–7194 (2019).

[29] Z. A. Piskulich and W. H. Thompson, "On the temperature dependence of liquid structure," J. Chem. Phys. **152**, 011102 (2020).

[30] Z. A. Piskulich and W. H. Thompson, "The dynamics of supercooled water can be predicted from room temperature simulations ," J. Chem. Phys. **152**, 074505 (2020).

[31] Z. A. Piskulich and W. H. Thompson, "Temperature dependence of the water infrared spectrum: Driving forces, isosbestic points, and predictions," J. Phys. Chem. Lett. **11**, 7762–7768 (2020).

[32] D. E. Moilanen, E. E. Fenn, Y.-S. Lin, J. L. Skinner, B. Bagchi, and M. D. Fayer, "Water inertial reorientation: Hydrogen bond strength and the angular potential," **105**, 5295–5300 (2008).

[33] G. M. Gale, G. Gallot, F. Hache, N. Lascoux, S. Bratos, and J. C. Leicknam, "Femtosecond dynamics of hydrogen bonds in liquid water: A real time study," Phys. Rev. Lett. **82**, 1068–1071 (1999).

[34] R. Laenen, K. Simeonidis, and A. Laubereau, "Subpicosecond spectroscopy of liquid water in the infrared: Effect of deuteration on the structural and vibrational dynamics," J. Phys. Chem. B **106**, 408–417 (2002).

[35] D. Laage and J. T. Hynes, "On the molecular mechanism of water reorientation." J. Phys. Chem. B **112**, 14230–14242 (2008).

[36] D. M. Wilkins, D. E. Manolopoulos, S. Pipolo, D. Laage, and J. T. Hynes, "Nuclear quantum effects in water reorientation and hydrogen-bond dynamics," J. Phys. Chem. Lett. **8**, 2602–2607 (2017).

[37] J. Stenger, D. Madsen, P. Hamm, E. T. J. Nibbering, and T. Elsaesser, "Ultrafast vibrational dephasing of liquid water," Phys. Rev. Lett. **87**, 027401 (2001).

[38] C. J. Fecko, J. J. Loparo, S. T. Roberts, and A. Tokmakoff, "Local hydrogen bonding dynamics and collective reorganization in water: Ultrafast infrared spectroscopy of HOD/DO," J. Chem. Phys. **122**, 054506 (2005).

[39] J. B. Asbury, T. Steinel, C. Stromberg, S. A. Corcelli, C. P. Lawrence, J. L. Skinner, and M. D. Fayer, "Water dynamics: Vibrational echo correlation spectroscopy and comparison to molecular dynamics simulations," J. Phys. Chem. A **108**, 1107–1119 (2004).

[40] Y. Ni and J. L. Skinner, "Ultrafast pump-probe and 2DIR anisotropy and temperature-dependent dynamics of liquid water within the E3B model," Journal of Chemical Physics **141** (2014), 10.1063/1.4886427.

[41] K. Kwak, D. E. Rosenfeld, and M. D. Fayer, "Taking apart the two-dimensional infrared vibrational echo spectra: More information and elimination of distortions," J. Chem. Phys. **128**, 204505 (2008).

[42] O. O. Mesele and W. H. Thompson, "Removing the barrier to the calculation of activation energies," J. Chem. Phys. **145**, 13410 (2016).

[43]S. Plimpton, "Fast parallel algorithms for short-range molecular dynamics," J. Comput. Phys. **117**, 1–19 (1995).
[44]H. J. Berendsen, J. R. Grigera, and T. P. Straatsma, "The missing term in effective pair potentials," J. Phys. Chem **91**, 6269–6271 (1987).
[45]T. Darden, D. York, and L. Pedersen, "Particle mesh Ewald: An N·log(N) method for Ewald sums in large systems," J. Chem. Phys. **98**, 10089–10092 (1993).
[46]E. L. Pollock and J. Glosli, "Comments on PPPM, FMM, and the Ewald method for large periodic Coulombic systems," Comput. Phys. Comm. **95**, 93–110 (1995).
[47]J. P. Ryckaert, G. Ciccotti, and H. J. Berendsen, "Numerical integration of the cartesian equations of motion of a system with constraints: molecular dynamics of n-alkanes," Journal of Computational Physics **23**, 327–341 (1977).
[48]S. Nosé, "A unified formulation of the constant temperature molecular dynamics methods," J. Chem. Phys. **81**, 511–519 (1984).
[49]W. G. Hoover, "Canonical dynamics: Equilibrium phase-space distributions," Phys. Rev. A **31**, 1695–1697 (1985).
[50]K. Levenberg, "A method for the solution of certain non-linear problems in least squares," Q. Appl. Math. **2**, 164–168 (1944).
[51]D. W. Marquardt, "An algorithm for least-squares estimation of nonlinear parameters," Math., J. Soc. Indust. Appl. **11**, 431–441 (1963).
[52]D. P. Shoemaker, C. W. Garland, and J. W. Nibler, *Experiments in physical chemistry* (McGraw-Hill, New York, 1989).
[53]C. J. Tainter, P. A. Pieniazek, Y. S. Lin, and J. L. Skinner, "Robust three-body water simulation model," J. Chem. Phys. **134**, 184501 (2011).
[54]C. J. Tainter, L. Shi, and J. L. Skinner, "Reparametrized E3B (explicit three-body) water model using the TIP4P/2005 model as a reference," J. Chem. Theory Comput. **11**, 2268–2277 (2015).
[55]S. A. Corcelli, C. P. Lawrence, and J. L. Skinner, "Combined electronic structure/molecular dynamics approach for ultrafast infrared spectroscopy of dilute HOD in liquid H_2O and D_2O," J. Chem. Phys. **120**, 8107–8117 (2004).
[56]S. A. Corcelli and J. L. Skinner, "Infrared and Raman Line Shapes of Dilute HOD in Liquid H_2O and D_2O from 10 to 90°C," J. Phys. Chem. A **109**, 6154–6165 (2005).
[57]B. M. Auer and J. L. Skinner, "IR and Raman spectra of liquid water: Theory and interpretation," J. Chem. Phys. **128**, 224511 (2008).
[58]S. M. Gruenbaum, C. J. Tainter, L. Shi, Y. Ni, and J. L. Skinner, "Robustness of frequency, transition dipole, and coupling maps for water vibrational spectroscopy," J. Chem. Theor. Comp. **9**, 3109–3117 (2013).
[59]J. R. Schmidt, S. T. Roberts, J. J. Loparo, A. Tokmakoff, M. D. Fayer, and J. L. Skinner, "Are water simulation models consistent with steady-state and ultrafast vibrational spectroscopy experiments?" Chem. Phys. **341**, 143–157 (2007).
[60]S. A. Corcelli, C. P. Lawrence, J. B. Asbury, T. Steinel, M. D. Fayer, and J. L. Skinner, "Spectral diffusion in a fluctuating charge model of water." J. Chem. Phys. **121**, 88978900 (2004).
[61]P. C. Burris, D. Laage, and W. H. Thompson, "Simulations of the infrared, Raman, and 2D-IR photon echo spectra of water in nanoscale silica pores," J. Chem. Phys. **144**, 194709 (2016).
[62]S. Park, D. E. Moilanen, and M. D. Fayer, "Water dynamics–the effects of ions and nanoconfinement." J Phys Chem B **112**, 52795290 (2008).
[63]Our f-test for the FFCF gives a value of F=25.79 which is greater than the critical f-value of 3.85 corresponding to the present degrees of freedom and a 95% confidence interval, indicating that the 4-exponential fit is a statistically significant improvement over the 3-exponential fit. The corresponding f-test for the fit of the derivative FFCF gives a value of F=1802.86, which is again greater than the critical f-value.
[64]This is true even if one assumes that the spectral diffusion time is obtained from the sum of forward and backward exchange rate constants, *i.e.*, $1/\tau_\omega = k_\omega = k_f + k_b$. That is, it is straightforward to show that $E_{a,\omega} = -\partial(\ln k_\omega)/\partial\beta = (k_f/k_\omega)E_{a,f} + (k_b/k_\omega)E_{a,b}$. Then, assuming the forward and backward H-bond exchange processes have the same rate constant and activation energies by symmetry, namely the values associated with the H-bond jump time, $k_f = k_b = 1/\tau_0$ and $E_{a,f} = E_{a,b} = E_{a,0}$, it is clear that $E_{a,k} = E_{a,0}$.
[65]We have verified, for the SPC/E model, that an Arrhenius analysis over a narrow temperature range (290, 298.15, and 310 K) gives a spectral diffusion activation energy ($E_a = 2.61 \pm 0.21$ kcal/mol) in agreement with our value directly calculated from simulations at 298.15 K ($E_a = 2.24 \pm 0.51$ kcal/mol).
[66]R. A. Nicodemus, K. Ramasesha, S. T. Roberts, and A. Tokmakoff, "Hydrogen bond rearrangements in water probed with temperature-dependent 2D IR," J. Phys. Chem. Lett. **1**, 1068–1072 (2010).
[67]R. A. Nicodemus, S. A. Corcelli, J. L. Skinner, and A. Tokmakoff, "Collective hydrogen bond reorganization in water studied with temperature-dependent ultrafast infrared spectroscopy," J. Phys. Chem. B **115**, 5604–5616 (2011).
[68]F. Perakis and P. Hamm, "Two-dimensional infrared spectroscopy of supercooled water," J. Phys. Chem. B **115**, 5289–5293 (2011).
[69]R. C. Tolman, "Statistical mechanics applied to chemical kinetics," J. Am. Chem. Soc. **42**, 2506–2528 (1920).
[70]D. E. Moilanen, D. Wong, D. E. Rosenfeld, E. E. Fenn, and M. D. Fayer, "Ion-water hydrogen-bond switching observed with 2d ir vibrational echo chemical exchange spectroscopy." Proc Natl Acad Sci U S A **106**, 375380 (2009).
[71]G. Stirnemann, J. T. Hynes, and D. Laage, "Water hydrogen bond dynamics in aqueous solutions of amphiphiles," J Phys Chem B **114**, 30523059 (2010).